



Madhlopa, A. and Ngwalo, G. (2007) Solar dryer with thermal storage and biomass backup heater. *Solar Energy*, 81 (4). pp. 449-462. ISSN 0038-092X

<http://strathprints.strath.ac.uk/16428/>

This is an author produced version of a paper published in *Solar Energy*, 81 (4). pp. 449-462. ISSN 0038-092X. This version has been peer-reviewed but does not include the final publisher proof corrections, published layout or pagination.

Strathprints is designed to allow users to access the research output of the University of Strathclyde. Copyright © and Moral Rights for the papers on this site are retained by the individual authors and/or other copyright owners. You may not engage in further distribution of the material for any profitmaking activities or any commercial gain. You may freely distribute both the url (<http://strathprints.strath.ac.uk>) and the content of this paper for research or study, educational, or not-for-profit purposes without prior permission or charge. You may freely distribute the url (<http://strathprints.strath.ac.uk>) of the Strathprints website.

Any correspondence concerning this service should be sent to The Strathprints Administrator: eprints@cis.strath.ac.uk

Solar dryer with thermal storage and biomass backup heater

A. Madhlopa^{a,*} G. Ngwalo^b

^a Department of Physics and Biochemical Sciences,

^b Department of Mechanical Engineering, Malawi Polytechnic, P/Bag 303, Blantyre 3, Malawi.

Abstract

An indirect type natural convection solar dryer with integrated collector-storage solar and biomass backup heaters has been designed, constructed and evaluated. The major components of the dryer are biomass burner (with a rectangular duct and flue gas chimney), collector-storage thermal mass and drying chamber (with a conventional solar chimney). The thermal mass was placed in the top part of the biomass burner enclosure. The dryer was fabricated using simple materials, tools and skills, and it was tested in three modes of operation (solar, biomass and solar-biomass) by drying twelve batches of fresh pineapple (*Ananas comosus*), with each batch weighing about 20 kg. Meteorological conditions were monitored during the dehydration process. Moisture and vitamin C contents were determined in both fresh and dried samples. Results show that the thermal mass was capable of storing part of the absorbed solar energy and heat from the burner. It was possible to dry a batch of pineapples using solar energy only on clear days. Drying proceeded successfully even under unfavorable weather conditions in the solar-biomass mode of operation. In this operational mode, the dryer reduced the moisture content of pineapple slices from about 669 to 11% (db) and yielded a nutritious dried product. The average values of the final-day moisture-pickup efficiency were 15, 11 and 13% in the solar, biomass and solar-biomass modes of operation respectively. It appears that the solar dryer is suitable for preservation of pineapples and other fresh foods. Further improvements to the solar chimney design are suggested to avert reverse thermosiphoning at night or during periods of low insolation.

Key words: Natural convection, thermal storage, efficiency.

1. Introduction

Dehydration is a common technique for preservation of agricultural and other products, including fruits and vegetables. In developing countries, the traditional method of dehydration is by open air, which often results in food contamination and nutritional deterioration (Ratti and Mujumdar, 1997). Some of the problems associated with open-air drying can be solved through the use of solar dryers which are generally classified, depending on the mode of heating or operation, into: a) direct, b) indirect and, c) mixed mode systems with natural or forced circulation of the drying air. In the direct

* Corresponding author: Fax: 265 1 670 578, e-mail: amadhlopa@poly.ac.mw

dryer, solar radiation passes through a transparent cover fitted on the top part of the dryer and is directly absorbed by the crop placed on the drying bed under the transparent cover. In an indirect dryer, air is heated in a separate solar collector and circulated through the drying bed where it picks moisture from the crop. The mixed mode possesses both features of the direct and indirect categories of solar dryers. In particular, dryers of the natural-convection variety are popular because they are cheap and simple to operate and maintain (Soponronnarit, 1995). They exhibit enormous potential for exploitation in remote areas of developing countries, where most of the rural communities have no access to electricity. Nevertheless, one disadvantage of solar drying is that the dehydration process is interrupted at night or under low insolation, resulting in a poor quality of the dried product.

Several attempts have been made to overcome the problem of intermittent drying in natural convection solar drying. One approach has been the use of thermal storage. Khanna (1967) studied design data for solar heating of air using a heat exchanger (heat transfer by both natural and forced modes). It was found that the data would assist in obtaining the final design of a shell-and-tube heat exchanger for use in drying a specific material. Ayensu and Asiedu-Bondzie (1986) constructed a dryer with thermal storage, from locally available materials. The system was capable of transferring 118 W m^{-2} to the drying air. Ayensu (1997) designed and constructed a solar dryer with a rock storage system. It was found that the rock pile stored enough energy to enhance nocturnal drying. The duration of crop drying in the solar dryer was shorter than that in the open air. Aboul-Enein et al. (2000) developed a solar air heater and tested it with and without thermal storage for drying agricultural products. They found that the drying process would continue at night when a thermal mass was used. El-Sebaai et al. (2002) developed a solar dryer with a thermal storage system. The dryer was tested with and without thermal storage. They found that the storage material reduced the drying period. Enibe (2002) used a phase change material to store thermal energy in a solar air heating system. It was found that the system could be operated for crop drying and poultry egg incubation. In all these studies, solar energy was used exclusively. However, the intensity of solar radiation is sometimes so low that the temperature of the thermal mass may rise by an insignificant margin above the ambient level, and thereby limiting the continuity of dehydration. There is, therefore, still need to backup the drying process in solar dryers with thermal mass.

Akyurt and Selçuk (1973) developed an indirect solar dryer with a backup gas burner. They found that the drying time could be shortened due to the inclusion of the backup heater. Bassey et al. (1987) used a sawdust burner to provide heat to a direct type solar dryer during bad weather and at night. In their study, the burner was not integrated to the dryer but used steam as a heat transfer medium. Bena and Fuller (2002) designed a direct solar dryer with an integrated biomass

backup heater. The thermal performance of their system was satisfactory. Prasad and Vijay (2005) also developed a direct solar-biomass dryer. The biomass burner has a rock slab on the top part which helps in moderating the temperature of the drying air. These dryer designs have a backup heater without thermal storage of captured solar energy. Consequently, the air temperature in the drying chamber drops down to ambient level immediately after sunset, requiring backup heating even when the preceding day is sunny. This leads to wastage of both solar and fuel resources.

Biomass (especially fuelwood) is a dominant source of energy, and commonly burned using inefficient technologies in most developing countries (Kristoferson and Bokalders, 1991; Bena and Fuller, 2002; Kaygusuz and Türker, 2002). So long this resource is harvested sustainably, it can provide the required backup thermal energy for solar drying in developing countries. However, information is scarce on solar drying with integrated collector-storage solar and biomass-backup heaters.

In this study, an indirect type natural convection solar dryer with integrated collector-storage solar and biomass backup heaters was developed. The absorber of the solar air heater was a horizontal concrete structure integrated to a rock bed. The backup heater was integrated to the solar collector and operated on wood shavings. The dryer was tested in three operational modes (solar, biomass and solar-biomass) by drying fresh pineapples (*Ananas comosus*) outdoors under different weather conditions. Results show that the dryer is capable of reducing the moisture content of pineapple slices to acceptable levels, and retaining part of the vitamin C in the slices. The drying process is fastest in the solar-biomass mode of operation while the efficiency of the dryer is most satisfactory in the solar mode. Other results are presented and discussed.

2. Design and construction

2.1 Solar collector, drying chamber and chimney

An indirect solar dryer was designed and constructed with a biomass backup burner (Figs. 1-3). The dryer has a solar collector, drying cabinet and backup heater. The size of the collector was based on meteorological and crop parameters. To dehydrate a fresh food with an initial mass (m_1), the required mass of dry air (m_a) to vaporize water (m_w) from the fresh food can be calculated by (Ayensu, 1997):

$$m_w = m_1(M_1 - M_2)/(100 - M_2) \quad (1)$$

$$m_a = m_w/(W_2 - W_1) \quad (2)$$

The thermal power (q) required for heating air is given by (ASHRAE, 2001):

$$q = F_a(h_p - h_i) \quad (3)$$

It can be shown, using Eq.(3), that the collector aperture area (A) required to capture the total amount of thermal energy in time τ is:

$$A = m_a(h_p - h_i) / (\eta_t H_d) \quad (4a)$$

$$H_d = \int_{\tau_1}^{\tau_2} I d\tau \quad (4b)$$

The solar system under discussion was designed to dehydrate 20.0 kg of pineapples in 259200 s, under the prevailing meteorological and food conditions shown in Table 1, with an assumed thermal efficiency $\eta_t = 0.24$. From Eq. (2), the mass of water evaporated in 259200 s is about 16.7 kg. Using psychrometric principles, ambient air is heated from point A (temperature $T_a = 303$ K, relative humidity $\phi = 80$ %, specific volume $v_s = 0.89$ m³ kg⁻¹) to point B ($T_p = 313$ K, $\phi = 47$ %) at constant humidity ratio (W) as shown in Fig. 4. The heated air (in plenum) passes through the drying bed and picks up moisture from the fresh food at constant enthalpy, increasing W from 0.0216 to 0.0272 kg/kg of dry air at point C where it is assumed saturated at $\phi = 90$ % and $T = 305$ K above the drying bed. Under these meteorological conditions (Table 1), $A = 2.2$ m², and the mass flow rate of dry air is 0.0115 kg s⁻¹. The collector of the dryer has a horizontal concrete absorber that is painted matt black on its top part and integrated to the rock pile (Fig. 3). It is enclosed in a wooden frame (constructed from block board, 0.02 m thick) mounted on the top part of the brick wall that houses the burner using metal straps mortared into the top part of the brick wall. The exterior part of the vertical faces of the collector was covered with a painted galvanized iron sheet (6 x 10⁻⁴ m thick) to protect the wood from weathering.

The standard storage capacity of a solar air heater is 0.25 m³ of pebbles (including void space) per unit area of the collector (Duffie and Beckman (1991)). For $A=2.2$ m² in the present study, the required pebble volume and depth would be about 0.55 m³ and 0.14 m respectively. However, the pebble bed (granite rock pebbles of about 0.025 m diameter) in this study has a horizontal concrete layer on its top part to augment the path length of the hot drying air from the external surface of the drum through the horizontal rock matrix before rising into the drying chamber via a rectangular hole (1.00 m x 0.09 m) at the front of the absorber. This flow pattern of hot air would enable a reasonable amount of heat from the biomass burner to be transferred to the thermal mass, thereby averting burning up of the drying product. It should also be noted that, during solar collection, heat is mainly transferred from the absorber plate to the rock bed by conduction because hot air is in the upper part of the bed. In view of the foregoing discussion, a slightly smaller

thickness (0.10 m) of the horizontal rock-and-concrete bed was used. A single glass cover was fitted on the top part of the collector and inclined at 16° to the horizontal with the system facing north to optimize solar collection at the Malawi Polytechnic (15° 48' S, 35° 02' E).

The drying chamber was also constructed from block board (0.02 m thick) and covered with a painted galvanized iron sheet (6 x 10⁻⁴ m thick). It accommodates three trays, each with a plastic mesh base, which slide horizontally along wooden rails fixed to the vertical sides of the cabinet. These trays have an effective area of 4.1 m², accommodate about 20 kg of fresh pineapple and can be removed for cleaning. The top surface of the cabinet is opaque, and inclined at 16° to the horizontal to facilitate drainage of rain water and flow of air from the plenum through the drying bed into the venting systems. Two wooden doors (1.20 m x 1.51 m), with an air vent (rectangle of 0.51 m by 0.10 m with semicircles on both short vertical sides) on the top part of each door, were fitted at the back of the chamber for accessing the trays. A wire mesh was fitted on the vents to keep away insects and rodents. In addition, an overhang was fitted over the outlet-air vents to prevent raindrops from entering the drying chamber through the vents, and a solar chimney was fitted on top of this chamber to increase natural convection of the drying air. The chimney was also made from a galvanized iron sheet (6 x 10⁻⁴ m thick) and painted matt black. The chamber was integrated to the collector. Some steps were constructed on the southern side of the system for ease of product loading and off-loading. Drying air enters the system through a rectangular inlet (1.00 m x 0.09 m) with a wire mesh, at the bottom part of the brick wall and gets into contact with the bare exterior part of the drum, without mixing with the flue gas. The heated air rises, by natural convection, into the drying chamber through another rectangular hole (1.00 m x 0.09 m) on the concrete absorber (location E in Fig.3). It passes through the drying bed (of effective thickness H_{dd} ≈ 0.3 m) and exits through a solar chimney or air outlet vents on the top part of the doors to the drying chamber.

Air flow is induced by the difference between temperatures of air in the system components and ambient air (Fig.5).

The thermal buoyancy (ΔP) in the system components is given by (Bala and Woods, 1994):

$$\Delta P = g\beta\rho_a(\Delta TH) \quad (5)$$

$$T_{ch} = T_a + (T_{co} - T_a)(1 - \exp(-R))/R \quad (6)$$

$$R = \pi D_{sc} U_L Z / (F_a C_a) \quad (7)$$

The total thermal buoyancy of the drying air (ΔP_{ta}) was found by summing up the contribution from the major components of the dryer shown in Fig. 4: burner enclosure (bu), collector (co), drying bed (dd) and solar chimney (sc).

$$\Delta P_{ta} = \Delta P_{bu} + \Delta P_{co} + \Delta P_{dd} + \Delta P_{sc} \quad (8)$$

There is resistive pressure (ΔP_{ra}) within the air passage components:

$$\Delta P_{ra} = 0.5\rho_a (K_{bu} + K_{co} + K_{sc})U^2 + K_{dd}U \quad (9)$$

The coefficients K_{bu} , K_{co} and K_{sc} were computed according to ASHRAE (2001), assuming the a) burner enclosure is rectangular, b) collector is an asymmetric diffuser (because the glass cover is inclined to absorber), c) chimney is cylindrical, and d) flow of air is viscous and fully-developed.

As the drying air leaves the burner enclosure, it passes through a narrow horizontal rectangular slot, resulting in contraction and pressure loss. In the collector, the drying air flows from a narrower cross-sectional area to a wider section at the exit from the collector resulting in air expansion and pressure loss. These losses are included in the computation of pressure loss coefficients.

$$K_{bu} = f_{bu}H_{bu}/D_{bu} + K_c \quad (10)$$

Where K_c accounts for pressure loss during contraction and is computed according to Miller (1979).

$$K_{co} = f_{co}L_{co}/D_{co} + K_e \quad (11)$$

K_e was computed according to (ASHRAE, 2001) for air flowing from a narrow section into a room, while K_{sc} was calculated by (Bala and Woods, 1994; ASHRAE, 2001):

$$K_{sc} = f_{sc}H_{sc}/D_{sc} \quad (12)$$

For laminar flow, the friction factor f can be calculated from (Bala and Woods, 1994; ASHRAE, 2001):

$$f = 64/Re \quad (13a)$$

$$Re = u_r D / \nu \quad (13b)$$

where u_r is a reference velocity in a given system component.

In this study, u_r was calculated from the mass flow rate obtained by psychrometric analysis:

$$u_r = v_s F_a / A_c \quad (14)$$

where A_c is the area of the reference cross-section in a component.

K_{dd} was calculated from the correlation reported by Ayensu (1997). System drying air velocity (U) was found by equating the total thermal buoyancy to resistive pressure (Bala and Woods, 1994; 1995):

$$\Delta P_{ta} = 0.5\rho_a (K_{bu} + K_{co} + K_{sc})U^2 + K_{dd}U \quad (15)$$

For $D_{sc} = 0.18$ m, the solar chimney height H_{sc} was theoretically varied from 1.0 to 2.0 m. It was found that U varied from 0.0333 to 0.0410 $m\ s^{-1}$, with corresponding volume flow rates of 0.0455 to 0.0560 $m^3\ s^{-1}$ through the drying bed. This range of air flow rate would be adequate for drying under the design weather conditions.

2.2 Biomass back up heater

In case of low solar irradiation during the day, the drying process can be backed up by a biomass heater. In this study, the backup heater was made of a drum, rectangular duct and flue gas chimney. The drum has a horizontal baffle and mild steel grill. The baffle is 0.06 m above the grill while the grill is fitted 0.20 m above the bottom part of the drum. A truncated circular removable lid was tightly-fitted on the open end of the drum through which biomass was loaded into and ash removed from the drum, with a rectangular steel door (with a cavity, 0.025 m thick and filled with vermiculite) fitted on the outer side of the lid. The door was perforated (total area of perforation = 3.55×10^{-3} m^2) in the bottom part for inlet of air into the combustion chamber (drum). The size of the perforated area was based on the estimated volume flow rate of air required for combustion. The drum was integrated to a rectangular duct (0.98 m x 0.48 m x 0.16 m) with 3 vertical baffles spaced at equal intervals to increase the path length of the flue gas and the amount of heat transferred to the drying chamber. Round steel bars (0.016 m diameter) were placed across the drum and duct at 0.3 m apart, and an expanded metal placed on top of the bars.

To design the flue gas chimney, it was assumed that 8 kg of biomass would be required to back up the drying process for about 43200 s from sunset to sunrise the next day. The required mass of air for complete combustion of the fuel (20 % excess air) and the mass of flue gas produced were calculated according to ASHRAE (2001). The flue gas flows through the drum, rectangular duct and exits through the flue gas chimney. The thermal power lost (q_{gf}) to ambience through the flue gas is given by (ASHRAE, 2001):

$$q_{fg} = F_{fg} C_{fg} (T_{fe} - T_a) \quad (16)$$

Eq. (16) shows that decreasing the flue gas exit temperature (T_{fe}) reduces q_{fg} . One way of achieving this is by increasing the resistive pressure (ΔP_{rf}) to flue gas flow induced by thermal buoyancy in different components of the flue gas circuit. In the present work, the major contributor of thermal buoyancy (ΔP_{tf}) is the flue gas chimney because the drum and the rectangular duct are horizontal. ΔP_{tf} was calculated as for ΔP_{ta} , with T_{co} substituted by T_{fe} .

$$\Delta P_{rf} = 0.5(K_{dr} + K_{du} + K_{fc}) \rho_a V^2 \quad (17)$$

where K_{dr} is the sum of the pressure loss coefficients of friction experienced by the flue gas as it leaves the drum (wide) and enters the rectangular duct (narrow), K_{du} is the sum of the pressure loss coefficients of friction and bends (assumed right-angled for laminar flow) within the duct, and K_{fc} is the pressure loss coefficient of friction in the chimney. These coefficients were computed as for the solar mode of operation, with a reference velocity (v_r) of the flue gas in a component calculated from F_{fg} . The velocity of the flue gas was calculated from:

$$\Delta P_{if} = 0.5(K_{dr} + K_{du} + K_{fc}) \rho_a V^2 \quad (18)$$

The height of the flue gas chimney was theoretically varied from 2 to 3 m for $D_{fc} = 0.12$ m and $T_{fc} = 353$ K. It was observed that V increased from 0.2350 to 0.2824 m s⁻¹, with corresponding volume flow rates through the drum increasing from 0.0621 to 0.0726 m³ s⁻¹, which was adequate for the required volume flow rate of air for fuel combustion in the drum. It was also necessary for the flue gas chimney to be discharging the flue gas above the drying chamber to prevent filtration of smoke into the drying chamber. Consequently, the height of the flue gas chimney was set at 2.12 m. The chimney (constructed from a galvanized iron sheet, 6 x 10⁻⁴ m thick) was fitted to the duct, and a hole was drilled at the bottom of the knee bend into the chimney to drain out flue-gas condensate from the system (ASHRAE, 2001). The biomass burner was enclosed in a brick wall (2.52 m x 1.55 m) with a cavity (0.05 m thick) which was filled with vermiculite to reduce heat loss through the wall.

3. Experimentation

3.1 Sample fruit and preparation

Pineapples are an important crop in tropical countries. They are eaten fresh or mostly canned into juice and other products (Tanaka et al., 1999). However, technologies for canning or storing fresh fruits are very limited in developing countries. In addition, farmers face problems of shipping fresh fruits from rural areas to potential markets in urban areas of these countries, resulting in spoilage of the fresh produce and economic loss. Solar drying can be employed in remote areas to preserve harvested pineapples for local consumption or safe distribution.

In the present study, twelve batches of fresh pineapples were procured from a produce market. The fruits were washed, peeled, sliced (disc-shaped slices, thickness of about 0.01 m) and cored. For each batch, the slices were weighed on a digital top-loading balance (Adam Equipment co., model ACW-6) and loaded into the dryer for dehydration, with one layer on each tray.

3.2 Operational modes

The dryer was tested outdoors in three different operational modes: solar, biomass and a combination of the two energy sources. For the solar mode of operation, a batch of fresh pineapple slices was weighed, loaded into the dryer in the morning and re-weighed after 86400 s and on the final day of drying. For the biomass mode of operation, drying of a batch started in the evening. The aperture of the dryer was covered with a ceiling board (a black polythene paper was pasted on the top part of the board) which was parallel to and extended by 0.6 m beyond the perimeter on all sides of the glass cover, with an air gap of 0.6 m between the board and the transparent cover (ASHRAE, 1988). To block radiation when the altitude of the sun was low, a vertical removable ceiling board (wrapped in a black polythene paper) was fitted on the eastern side in the morning and western side of the collector in the afternoon. The location of this shield was changed around solar noon and immediately after sunset. The burner was charged with 8 kg of wood shavings and ignited around sunset. Again, the batch was re-weighed after 86400 s of drying. Due to lack of automated instrumentation for recording temperatures at night, the burner was charged with biomass fuel at sunrise, with the solar aperture covered, to establish the maximum levels of plenum temperatures. The door to the biomass burner was opened or closed to control the rate of combustion. For the solar-biomass mode, the burner was again charged once with the biomass fuel around sunset, and the samples were re-weighed after 86400 s and on the final day of drying.

3.3 Measurement of meteorological variables

Twelve mercury-in glass thermometers were inserted horizontally into the dryer (six on the eastern side and six on the western side of the drying chamber). On each side, three of the thermometers measured the plenum air temperature (below the drying bed) while the other three measured the temperature of the air above the drying bed. At the end of a drying run, the temperature of the top part of the thermal mass was also measured at five different locations (at the four corners and middle of the concrete absorber). Ambient air temperature was monitored by using a mercury-in glass thermometer placed in a room with open louvers to allow free circulation of air. Flue gas temperature was also monitored using a mercury in-glass thermometer. A wet and dry bulb thermometer (Kagaka Kyoeisha, model SLLB) was used to measure the level of relative humidity while wind velocity was measured by a Casella low-speed air meter (N 1462). The flow rate of drying air through the dryer was measured by placing the air meter in the middle of the air inlet to the drying chamber (position E in Fig. 3), with the air vented through the solar chimney. The intensity of global solar radiation was measured by a Kipp & Zonen pyranometer (CM 6B) mounted in the plane of the transparent cover, and connected to a Kipp & Zonen solar integrator (CC 14).

3.4 Physico-chemical analysis

The moisture content of fresh and dried samples was determined by drying an accurately-weighed (5 g) sample in an electric oven (Griffin, serial number 0518171070) at 343 K for 21600 s (AOAC, 1990). The loss in moisture was calculated as a percentage of the mass of the dry sample. The uniformity of drying at different levels of the trays was determined by weighing all the pineapple slices from each tray. In addition, five samples were taken from different positions of each tray to establish the uniformity of drying across the tray (Fig.7).

Early studies indicate that vitamin C is particularly vulnerable to destruction under different conditions (air, light and heat) and during processing (Drew and Ree, 1980; Fellows and Hampton, 1992). So, the retention of vitamin C is used as a good indicator of the preservation of all other nutrients (Maeda and Salunkhe, 1981). Consequently, the retention of vitamin C was used as an indicator of nutritional quality in this study. The concentration of vitamin C in fresh and dried pineapple samples was determined according to AOAC (1990), and expressed on dry basis. The percentage retention (R_v) of vitamin C was computed by:

$$R_v = 100 V_d/V_w \quad (19)$$

where V_d is the concentration of vitamin C in dried samples on dry basis (kg/kg of sample), and V_w is the concentration of vitamin C in fresh samples on dry basis (kg/kg sample).

3.5 Data processing

During solar collection, the top part of the thermal mass absorber heats up faster than the bottom part. The thermal energy is conducted through the rock pile until an equilibrium state is established. During heat charging using the biomass heater, the bottom part of the thermal mass heats up faster than the top part until equilibrium temperatures are again established. However, due to lack of suitable instruments for measuring temperature in the bottom part of the storage unit, only temperatures on the top part were monitored. In view of this, the temperatures on the bottom part of the thermal mass were found by calculation.

Heat (q_{at-as}) is conducted from the top surface of the concrete absorber plate ($T = T_{at}$) to the interface ($T = T_{as}$) between the absorber plate and the rock matrix, and heat (q_{as-st}) is conducted from the interface to the bottom of the rock pile ($T = T_{st}$). In a steady state, the rate of heat transfer from the interface to the bottom of the rock pile is equal to the rate of heat loss from the bottom of the rock bed (Fig.6). The heat balance can be represented by the following equations, assuming heat conduction is one-dimensional:

$$q_{at-as} = q_{as-st} \quad (20)$$

$$q_{as-st} = q_{c,st-a} + q_{r,st-bo} + q_{r,st-wa} \quad (21)$$

$$q_{r,st-bo} = q_{bo-gr} \quad (22)$$

$$q_{r,st-wa} = q_{wa-a} \quad (23)$$

$$q_{at-as} = k_{ab}A_{ab}(T_{at} - T_{as})/x_{ab} \quad (24)$$

$$q_{as-st} = k_sA_s(T_{as} - T_{st})/x_s \quad (25)$$

$$q_{c,st-a} = A_{st}h_{c,st-a} (T_{st} - T_a) \quad (26)$$

$$q_{r,st-bo} = h_{r,st-bo} (T_{st} - T_{bo}) \quad (27)$$

$$q_{r,st-wa} = h_{r,st-a} (T_{st} - T_{wa}) \quad (28)$$

$$q_{wa-a} = [2x_{wa}/(A_{wa}k_{wa}) + x_{ve}/(A_{wa}k_{ve})]^{-1}(T_{wa} - T_a) \quad (29)$$

$$q_{bo-gr} = k_{bo}A_{bo}(T_{bo} - T_a)/x_{bo} \quad (30)$$

All the coefficients of heat transfer were computed according to (Incropera and DeWitt, 2002), assuming the a) rock bed is a horizontal plate cooled from the bottom, b) rock bed and the concrete base are parallel plates, and c) rock bed is perpendicular to the wall enclosing the burner (for calculation of view factors). Properties of air were calculated at $0.5(T_{st}+T_a)$. Eqs.(19-28) were solved simultaneously using the Gauss-Seidel iterative method to find T_{as} and T_{st} , with ground temperature assumed at ambient level (Duffie and Beckman, 1991). The total heat stored (q_{sr}) by the absorber concrete plate and rock bed was calculated as follows:

$$q_{sr} = m_{ab}C_{ab}(T_{ma} - T_a) + m_sC_s(T_{ms} - T_a) \quad (31a)$$

$$T_{ma} = 0.5(T_{at} + T_{as}) \quad (31b)$$

$$T_{ms} = 0.5(T_{as} + T_{st}) \quad (31c)$$

During biomass burning, the bottom part of the rock bed receives a relatively high quantity of heat through convection and radiation from the hot drum. So, the bottom part of the storage structure would be hotter than the top part of the absorber plate. In view of this, a similar computational procedure (to that for the solar mode of operation) was used with $T_{st} > T_{at}$ and the following additional heat balance equations:

$$A_{ab}k_{ab}(T_{as} - T_{at})/x_{ab} = (A_g h_{c,ab-g} + h_{r,ab-g})(T_{at} - T_g) + (A_{ab}h_{c,ab-da})(T_{at} - T_p) \quad (32)$$

$$(A_g h_{c,ab-g} + h_{r,ab-g})(T_{at} - T_g) = (A_g h_{c,g-a} + h_{r,g-a})(T_g - T_a) \quad (33)$$

Moisture-pickup efficiency (η_w) varies with the nature and moisture content of the fresh product. Unfortunately, there is lack of standard methods for testing solar dryers which adversely affects their evaluation (Sodha et al., 1987). So,

Leon et al. (2002) recommend the use of the first- and final-day efficiencies for evaluation of drying efficiency. In this study, η_w was computed by using the procedure reported by Bena and Fuller (2002) and Leon et al. (2002):

$$\eta_w = m_w h_{wg} / (A_{co} H_d + C_v m_b) \quad (34)$$

The calorific value of the biomass (C_v) was determined using a Gallenkamp automatic adiabatic bomb calorimeter (cat. no. 15 CB 110) and corrected for moisture content. The latent heat of vaporization (h_{wg}) was calculated using a temperature dependent function reported by Jannot and Coulibaly (1998), and increased by 15 % to include the extra energy required for evaporating moisture from biological materials (Hall, 1957):

$$h_{wg} = 2.5018 - 0.002378 (T_{wp} - 273.15) \quad (35)$$

The wet bulb temperature (T_{wp}) of the drying air in the plenum was computed using the procedure recommended by ASHRAE (1994).

4. Results and discussion

4.1 Weather conditions

Table 2 shows the variability of average weather conditions during the dehydration of a typical batch of fresh pineapple slices. The weather was favorable on some of the days. The levels of relative humidity ranged from 76 % to 82 %, with mean ambient air temperatures varying between 288 and 290 K. It is seen that the daily global solar radiation on an inclined plane (16° to the horizontal) was variable, ranging from 8.4×10^6 to $2.16 \times 10^7 \text{ J m}^{-2}$. These weather conditions indicate that drying would not proceed quickly on some days if a biomass backup heater was not used. However, the daily intensity of solar radiation was quite high on some days (typically $3.07 \times 10^7 \text{ J m}^{-2}$ on 22nd November 2004), which shows the potential for using the dryer without backup heating under sunny weather conditions.

4.2 Air and flue gas temperature

The plenum air passes through the drying bed where it picks up moisture from the drying food by natural convection. Figs. 8 (a-d) show the variation of mean plenum and ambient air temperatures on typical days of drying. For the solar mode of operation, it is seen that the plenum and ambient temperatures are almost equal in the morning but different during the day. In particular, the plenum temperature is higher than the ambient temperature during most of the day. The plenum-ambient temperature difference (excess temperature) was 17 K at 13:00 h, about 3600 s behind the time when the maximum solar irradiation was observed. The excess temperature was 12 K at 17:00 h and it dropped down to 0 K by the next morning. This indicates that the dryer stored part of the captured solar energy (stored energy $q_{sr} \approx 11.7 \times 10^6 \text{ J}$). A similar trend of the plenum temperature was observed on other sunny days. Leon et al. (2002) report

that a temperature difference (between ambient and drying air) of at least 10 K is required for drying to continue. This shows that drying continued even after sunset.

For the biomass mode of operation, the plenum temperature was initially monitored without any fire in the burner. It was found that there was insignificant difference between the plenum and ambient temperatures during the day, which indicated that the insulation cover over the solar collector was effective in blocking off irradiation during the day.

When the burner was charged in the morning, it was observed that the combustion process proceeded for about 36000 and 21600 s with the burner door closed and open respectively, which indicates that closing the burner door reduced the rate of combustion (The combustion process yielded grey ash, which is satisfactory). It is observed that the plenum temperature is higher than ambient temperature immediately after 06:00 to 17:00 h, with maximum values of 314 and 329 K on typical days shown in Figs. 8 (b-c)). There is an excess temperature of at least 10 K within the plenum for over 604800 s during the day. In particular, it should be noted that the excess plenum temperatures were 10 and 27 K with the burner door closed and open at 17:00 h respectively. This is attributed to the stored thermal energy ($q_{sr} \approx 9.0 \times 10^6$ and 1.86×10^7 J with the burner door closed and open respectively) which was released slowly into the plenum even after the completion of combustion. It is observed that leaving the burner door open leads to higher plenum temperatures. The flue gas temperature (T_g) was variable, with observed maxima of 326 and 383 K on typical days with closed and open burner door, respectively. A similar trend (higher values of T_g with open burner door) was observed on other test days, which is attributed to increased supply of excess air for combustion.

For the solar-biomass mode of operation, it is observed that the plenum temperature was higher than ambient temperature from 06:00 h to 17:00 h (stored biomass energy = 1.02×10^7 J), with excess temperature increasing to a maximum value of 18 K around 09:00 h and 10:00 h, then dropping down to 7 K at 17:00 h. Moreover, the burner was re-charged with wood shavings at sunset. So, food dehydration proceeded satisfactorily during both day and night in this mode of operation.

4.3 Drying time and uniformity

For the solar mode of operation, it was found that the dryer reduced the moisture content of a typical batch of fresh pineapple slices from $669 \pm 24\%$ to $16 \pm 0\%$ (on dry basis, db) in 345600 to 432000 s, with the daily intensity of global solar radiation varying from 1.84 to 2.68×10^7 J m⁻² on an inclined plane (16° to the horizontal). It is observed that there was significant variation in the moisture content of fresh samples, probably due to the season and maturity stage of the

fruit. It should also be mentioned that the drying product was not removed daily from the dryer after sunset because the stored thermal energy enabled drying to proceed at night. So, the dryer can be exclusively powered by solar energy to dehydrate a fresh food to the required level of moisture under favorable weather conditions, thereby saving biomass fuel.

For the biomass mode of operation (with a non-irradiated collector), it was observed that the dryer reduced the moisture content of a batch from 614 ± 14 % (db) to 13 ± 0 % (db) in 259200 s. Again, there was significant variation in the moisture content of fresh samples. Prolonging the dehydration process to 302400 s resulted in an over-dried product. The rate of drying in this mode of dryer operation was higher than that of the solar mode, which is attributed to the higher amount of energy supplied by the wood shavings (measured $C_v = 1.76 \times 10^7$ J kg⁻¹) than that from the sun.

The solar-biomass mode of operation was used to study the time and uniformity of drying. Fig.9 shows the variation of the mass and moisture content of a typical batch of pineapples. It is observed that the rate of drying was highest during the first 86400 s, with the mass of the batch dropping from 20.01 kg to 12.28 kg. The mass of the sample was 2.90 kg after 259200 s, with negligible drying thereafter. It is seen that the moisture content dropped from 669 ± 24 % to 11 ± 0 % (db) in 259200 s, with the intensity of the daily global solar radiation varying from 1.52 to 2.15×10^7 J m⁻². It is again seen that there was significant variation in the moisture content of fresh samples. Lower final levels of moisture content can be achieved in shorter drying periods with higher intensities of global radiation. Leon et al. (2002) recommend a final moisture content of 10 % (wet basis, wb), which is equivalent to 11 % (db), for evaluation of solar dryers. It should also be mentioned that long drying periods contribute to loss of vitamin C (Negi and Roy, 2000). So, the final moisture level obtained after drying a batch of pineapple slices for 259200 s was within acceptable limits when the solar dryer was backed up by a biomass burner.

Fig.10 shows the rate of drying at different trays in the drying chamber. It is seen that samples in the bottom tray dried fastest, with the top tray exhibiting the least drying rate. This drying pattern is attributed to the moisture content of the drying air. Hot air from the collector starts picking moisture from the bottom tray (thereby increasing its humidity ratio) before reaching the middle and top trays. Consequently, it is necessary to swap the trays in order to ensure uniform drying.

The uniformity of drying across the bottom tray is shown in Fig.11. It is seen that samples from positions A and B (in front of the tray) dried fastest with those at positions C and D (back of tray) exhibiting the least drying rate. The middle sample (position O) exhibited an intermediate rate of drying. A similar pattern of drying uniformity was observed across the middle and top trays, with the drying rate being most non-uniform across the top tray. These observations are again attributed to the moisture content of the heated air as it passes through the drying bed. A similar drying pattern is expected for the solar and biomass operational modes.

4.4 Vitamin C

The concentration of vitamin C in fresh pineapples varied from 2.2 to 3.4×10^{-4} kg/kg (wb) of sample, with a mean value of $2.6 \pm 0.4 \times 10^{-4}$ kg/kg (wb). These results are in close conformity with findings ($2.0-4.0 \times 10^{-4}$ kg/kg, wb) of Moser (1991). The retention of vitamin C in dried pineapple samples varied from 26 to 44 %. Maeda and Salunkhe (1981) report vitamin C retention values of 0.4-24.4 % in four different vegetables dried using solar dryers with and without shade over the drying product. They observed that there was higher retention of vitamin C in a solar dryer with shade (indirect solar drying). Wang et al. (1992) found a vitamin C loss of 82 % in the course of drum-drying potatoes. The relatively high losses in vitamin C are ascribed to the high sensitivity of this type of vitamin to different processes (blanching, drying, sample preparation) and conditions (Drew and Ree, 1980; Fellows and Hampton, 1992). Consequently, the levels of vitamin C retention found in the present study are satisfactory.

4.5 Drying air flow

For diurnal operation with the loaded dryer, the estimated air flow rate measured from position E (Fig. 3) varied from 0.017 to $0.036 \text{ m}^3 \text{ s}^{-1}$ (mean value of $0.024 \pm 0.002 \text{ m}^3 \text{ s}^{-1}$) when the dryer was operated with the solar chimney and wind speed $< 2.0 \text{ m s}^{-1}$. Enibe (2002) found a maximum flow rate of 0.058 kg s^{-1} for a natural convection solar air heating system.

For nocturnal operation, it was observed that there was condensate on a small portion of the absorber area directly below the air inlet to the solar chimney. This was attributed to reverse flow at night when the chimney became cold and acted as a condenser for the warm (and humid) air rising up from the drying bed. In view of this, the entrance to the solar chimney was blocked with card board papers at sunset (with air vents opened), and opened at sunrise (with air vents closed) to avert reverse thermosiphoning. This approach proved to be effective.

4.6 Dryer efficiency

Table 3 shows the first-day (η_1) and final-day (η_2) moisture-pickup efficiencies of the dryer (reported errors are standard). For the first-day efficiency, it is seen that the solar mode of operation exhibits the highest mean value, with the biomass mode showing the lowest value. This is probably due to the high heat losses through the flue gas, which results in a lower efficiency than that for the solar mode of operation. For the final-day efficiency, it is again observed that the system efficiency is highest (15 %), lowest (11 %) and intermediate (13 %) in the solar, biomass and solar-biomass modes of operation respectively. Brenndorfer et al. (1985) reports that typical efficiency values for a natural convection solar dryer are 10-15 %. Bena and Fuller (2002) report efficiency values of 22, 6 and 8.6 % for a direct type free-convection solar dryer operated in the solar, biomass and solar-biomass modes of operation respectively. Consequently, the performance of the present solar dryer is satisfactory.

5. Conclusion

An indirect type natural convection solar dryer has been designed and constructed with integrated thermal mass and biomass backup heater. Simple materials and skills were employed to build it. The dryer was tested in three modes of operation (solar, biomass and solar-biomass), using fresh pineapples under different weather conditions. Results show that the thermal mass stored part of the heat from both solar and biomass air heaters, thereby moderating temperature fluctuations in the drying chamber and reducing wastage of energy. Relatively high plenum temperatures were attained when the door to the biomass burner was kept open during the combustion period. It was possible to dry pineapple slices using solar energy only under favorable meteorological conditions. The solar mode of operation was slowest in drying the samples, with the solar-biomass mode being fastest under the prevailing meteorological conditions. Drying proceeded successfully even under very bad weather conditions in the solar-biomass mode of operation. Final moisture contents were within acceptable limits for safe storage of the dried pineapples which were also of high nutritional quality. The rate of drying was not uniform across the trays. Consequently, there is need for interchanging them during drying to achieve a uniformly-dried product. Reverse thermosiphoning was observed in the solar chimney during nocturnal drying, which reveals the need to re-visit the design of solar chimneys fitted on solar dryers developed for both diurnal and nocturnal drying of crops. The moisture-pickup efficiency of the system was most satisfactory in the solar mode of operation. It appears that the solar dryer is suitable for preservation of pineapples and other fresh foods. Nevertheless, the following further improvements are suggested: a) transparent insulation of the exterior surface of the solar chimney (or re-circulation of flue gas around the solar chimney) to avert reverse thermosiphoning at night or during periods of low insolation, and b) optimization of the system.

Nomenclature

A	area (m^2)
C	specific heat capacity of air at constant pressure ($\text{J kg}^{-1} \text{K}^{-1}$)
C_v	calorific value of biomass (Jkg^{-1})
D	diameter or hydraulic diameter (m)
f	friction factor in burner enclosure
F	fluid flow rate (kg s^{-1})
h	specific enthalpy (J kg^{-1})
h_c	convective heat transfer ($\text{W m}^{-2} \text{K}^{-1}$)
h_r	radiative heat transfer ($\text{W m}^{-2} \text{K}^{-1}$)
h_{wg}	latent heat of vaporization of water (J kg^{-1})
H	vertical height (m)
K	coefficient of pressure loss
k	coefficient of heat conductivity ($\text{W m}^{-2} \text{K}^{-1}$)
I	instantaneous solar irradiation (W m^{-2})
L	length (m)
m	mass (kg)
M	moisture content (%)
Nu	Nusselt number
q	thermal power (W)
ΔP	pressure drop (Pa)
Q	total thermal energy (MJ)
Re	Reynolds number
R_v	retention of vitamin C
T	temperature (K)
ΔT	difference between ambient and component air temperature (K)
u_r	reference air velocity (m s^{-1})
U	velocity of drying air (m s^{-1})
U_L	overall heat transfer coefficient from chimney ($\text{W m}^{-2} \text{K}^{-1}$)
V	velocity of flue gas (m s^{-1})

v_r	reference velocity of flue gas (m s^{-1})
v_s	specific volume of air ($\text{m}^3 \text{kg}^{-1}$)
V_d	concentration (db) of vitamin C in solar-dried sample (kg/kg of pineapple)
V_w	concentration (db) of vitamin C in fresh sample (kg /kg of pineapple)
W	humidity ratio (kg/kg of dry air)
x	thickness (m)
Z	height above drying bed as shown in Fig. 5, (m)

Greek letters

β	coefficient of thermal expansion
ν	kinematic viscosity ($\text{m}^2 \text{s}^{-1}$)
ϕ	relative humidity (%)
η	efficiency of dryer
ρ	air density (kg m^{-3})

Subscripts

1	initial
2	final
a	air/ambient
ab	absorber
at	absorber top part
b	biomass
da	drying air
bo	bottom concrete base
bu	burner
co	collector
dd	drying bed
db	dry basis
dr	drum
du	duct
fc	flue gas chimney
fe	flue gas exit from rectangular duct

i	inlet
ip	initial pineapple
p	plenum
pm	mean plenum
r	radiative
ra	resistance to drying air flow
rf	resistance to flue gas flow
s	storage bed
sc	solar chimney
sr	stored
st	rock storage bottom
t	thermal
ta	thermal buoyancy of drying air
tf	thermal buoyancy of flue gas
tm	thermal mass
ve	vermiculite
w	moisture/water
wa	wall
wb	wet basis
wp	wet bulb in plenum

Acknowledgements

The authors are very grateful to the National Research Council of Malawi for the financial support. The Malawi polytechnic is also acknowledged for the logistical and technical support.

References

- Aboul-Enein, S., El-Sebaei, Ramadan, M.R.I., El-Gohary, H.G., 2000. Parametric study of a solar air heater with and without thermal storage for solar drying. *Renewable Energy* 21, 505-522.
- Akyurt, M., Selçuk, M.K., 1973. A solar drier supplemented with auxiliary heating systems for continuous operation. *Solar Energy* 14, 313-320.

- AOAC, 1990. Official methods of analysis of the Association of Official Analytical Chemists, vol.2. AOAC, Inc., Virginia.
- ASHRAE, 1988. Methods of testing to determine the thermal performance of solar domestic water heating systems, standard 95-1987. American Society of Heating, Refrigerating and Air-conditioning Engineers, Atlanta.
- ASHRAE, 1994. Standard method for measurement of moist air properties, standard 41.6-94. American Society of Heating, Refrigerating and Air-conditioning Engineers Atlanta.
- ASHRAE, 2001. Fundamentals Handbook. American Society of Heating, Refrigerating and Air-conditioning Engineers, Atlanta.
- Ayensu, A., 1997. Dehydration of food crops using a solar dryer with convective heat flow. *Solar Energy* 59,121-126.
- Ayensu, A., Asiedu-Bondzie, V., 1986. Solar drying with convective self-flow and energy storage. *Solar & Wind Technology* 3, 273-279.
- Bala, B.K. and Woods, J.L., 1994. Simulation of the indirect natural convection solar drying of rice. *Solar Energy* 53, 259-266.
- Bala, B.K. and Woods, J.L., 1995. Optimization of natural convection, solar drying systems. *Energy* 20, 285-294.
- Bassey, M.W., Whitfield, M.J., Korama, E.Y., 1987 Problems and solutions for natural convection solar crop drying. In solar crop drying in Africa – Proceedings of food drying workshop, Dakar, Bassey M.W. and Schmidt O.G. (eds), IDRC, Ottawa, Canada.
- Bena, B., Fuller, R.J., 2002. Natural convection solar dryer with biomass backup heater. *Solar Energy* 72, 75-83.
- Brenndorfer, B., Kennedy, L., Bateman, C.O., Trim, D.S., Mrema, G.C., Wereko-Brobby, C., 1985. Solar dryers – Their role in post harvest processing. Commonwealth Science Council, London.
- Drew, F., Ree, K.I.S., 1980. Energy use, cost and product quality in preserving vegetables at home by canning, freezing and dehydration. *Food Science* 45, 1561-1565.
- Duffie, J.A. and Beckman, W.A., 1991. Solar engineering of thermal processes. John Wiley & Sons, Inc., New York, pp.393-399, 660-661.
- Enibe, O.S., 2002. Performance of a natural circulation solar air heating system with phase change material energy storage. *Renewable Energy* 27, 69-86.
- El-Sebaï, A.A., Aboul-Enein, S., Ramadan, M.R.I., El-Gohary, H.G., 2002. Experimental investigation of an indirect type natural convection solar dryer. *Energy Conversion and Management* 43, 2251-2266.
- Fellows, P., Hampton, A., 1992. Small-scale food processing: A guide to appropriate equipment. Intermediate Technology Publications, London, pp.3-9.

- Hall, W.C., 1957. *Drying farm crops*. Agricultural Consulting Associates, OH.
- Incropera, F.P., DeWitt, D.P., 2002. *Fundamentals of heat and mass transfer*, 5th ed. John Wiley & Sons, New York.
- Jannot, Y. and Coulibaly, Y., 1998. The “evaporative capacity as a performance” index for solar-drier air heater. *Solar Energy* 63, 387-391.
- Kaygusuz, K., Türker, M.F., 2002. Biomass energy potential in Turkey. *Renewable Energy* 26, 661-678.
- Khanna, M.L., 1967. Design data for solar heating of air using a heat exchange and storage system. *Solar Energy* 11, 142-144
- Kristoferson, L.K., Bokalders, V., 1991. *Renewable energy technologies: Their applications in developing countries*. Intermediate Technology Publications, Southmpton, pp. 3-19.
- Leon, M.A., Kumar, S., Bhattacharya, S.C., 2002. A comprehensive procedure for performance evaluation of solar food dryers. *Renewable and Sustainable Energy Reviews* 6, 367-393.
- Maeda, E.E., Salunkhe, D.K., 1981. Retention of ascorbic acid and total carotene in solar dried vegetables. *Food Science* 46, 1288-1290.
- Miller, D.S., 1978. *Internal flow systems*. British Hydromechanics Research Association Fluid Engineering, pp.260-278
- Moser, U., 1991. Vitamin C. In: Machlin, L.J. (ed.), *Handbook of vitamins*, 2nd ed. Marcel Dekker Inc., New York, pp.195-232.
- Negi, P.S., Roy, S.K., 2000. Effects of blanching and drying methods on β -carotene, ascorbic acid and chlorophyll retention of leafy vegetables. *Lebensm.-Wiss. u.-Technol.* 33, 295-298.
- Prasad, J., Vijay, V.K., 2005. Experimental studies on drying of *Zingiber officinale*, *Curcuma l.* and *Tinosopora cordifolia* in solar-biomass hybrid drier. *Renewable Energy* 30, 2097-2109.
- Ratti, C., Mujumdar, A.S., 1997. Solar dryer of foods: Modelling and Numerical simulation. *Solar Energy* 60, 151-157.
- Sodha, M.S., Bansal, N.K., Kumar, A., Bansal, P.K., Malik, A.E., 1987. *In solar crop drying*, vol II, CRC Press, Florida.
- Soponronnarit, S., 1995. Solar drying in Thailand. *Energy for Sustainable Development* 2, 19-25.
- Tanaka, K., Hilary, Z.D. and Ishzaki, A., 1999. Investigation of the utility of pineapple juice and pineapple waste material as low-cost substrate for ethanol fermentation by *Zymomonas mobilis*. *Bioscience and Bioengineering* 87, 642-646.
- Wang, X.Y., Kozempel, M.G., Hicks, K.B., Sieb, P.A., 1992. Vitamin C stability during preparation and storage of potato flakes and reconstituted mashed potatoes. *Food Science* 57, 1136-1139.

Table 1: Design parameters for a solar dryer with biomass back-up heater.

Dryer	Drying load and meteorological conditions
<p>Solar collector</p> <p>Aperture, $A = 2.2 \text{ m}^2$</p> <p>Absorber: Concrete slab (0.025 m thick)</p> <p>Glass cover</p> <p>Thickness = 3mm</p> <p>Tilt angle = 16°</p> <p>Granite rock = 360 kg</p> <p>Drying chamber</p> <p>Effective tray area = 4.1 m^2</p> <p>Solar chimney = 1.2 m height, 0.18 m ϕ</p> <p>Biomass burner</p> <p>Drum</p> <p>Length = 0.89 m</p> <p>Diameter = 0.58 m</p> <p>Door = 0.55 m x 0.54 m</p> <p>Flue gas Chimney</p> <p>Height = 2.12 m</p> <p>Diameter = 0.12 m</p>	<p>Drying product</p> <p>Initial mass of load, $m_1 = 20.0 \text{ kg}$</p> <p>Initial moisture, $M_1 = 85 \%$ (wet basis)</p> <p>Final moisture, $M_2 = 10 \%$ (wet basis)</p> <p>Meteorological conditions</p> <p>Solar radiation, $H_d = 6.30 \times 10^7 \text{ J m}^{-2}$</p> <p>Inlet air temperature = 303 K:</p> <p>Plenum temperature = 313 K</p> <p>Relative humidity, $\phi = 80 \%$</p>

Table 2: Weather conditions during one of the tests of the loaded solar dryer.

Date	Day or night	Weather	Mean ambient temperature (K)	Mean relative humidity (%)	Daily solar radiation ($\times 10^6 \text{ J m}^{-2}$)
1/6/04	Day	Partly cloudy with drizzles	290.15	78	16.6
1/6/04	Night	n.a.	288.15	n.a.	Nil
2/6/04	Day	Cloudy with showers	289.15	76	8.4
2/6/04	Night	n.a.	288.15	n.a.	Nil
3/6/04	Day	Partly cloudy	289.15	77	21.6
3/6/04	Night	n.a.	288.15	n.a.	Nil
4/6/04	Day	Cloudy with showers	289.15	82	13.5

Table 3: Variation of the first (η_{w1})- and final (η_{w2})-day moisture-pickup efficiencies.

Operational mode	Efficiency	
	η_{w1} (%)	η_{w2} (%)
Solar	20±2	15±1
Biomass	15±2	11±1
Solar-biomass	17±1	13±2



Fig.: 1: Perspective view of the solar dryer.

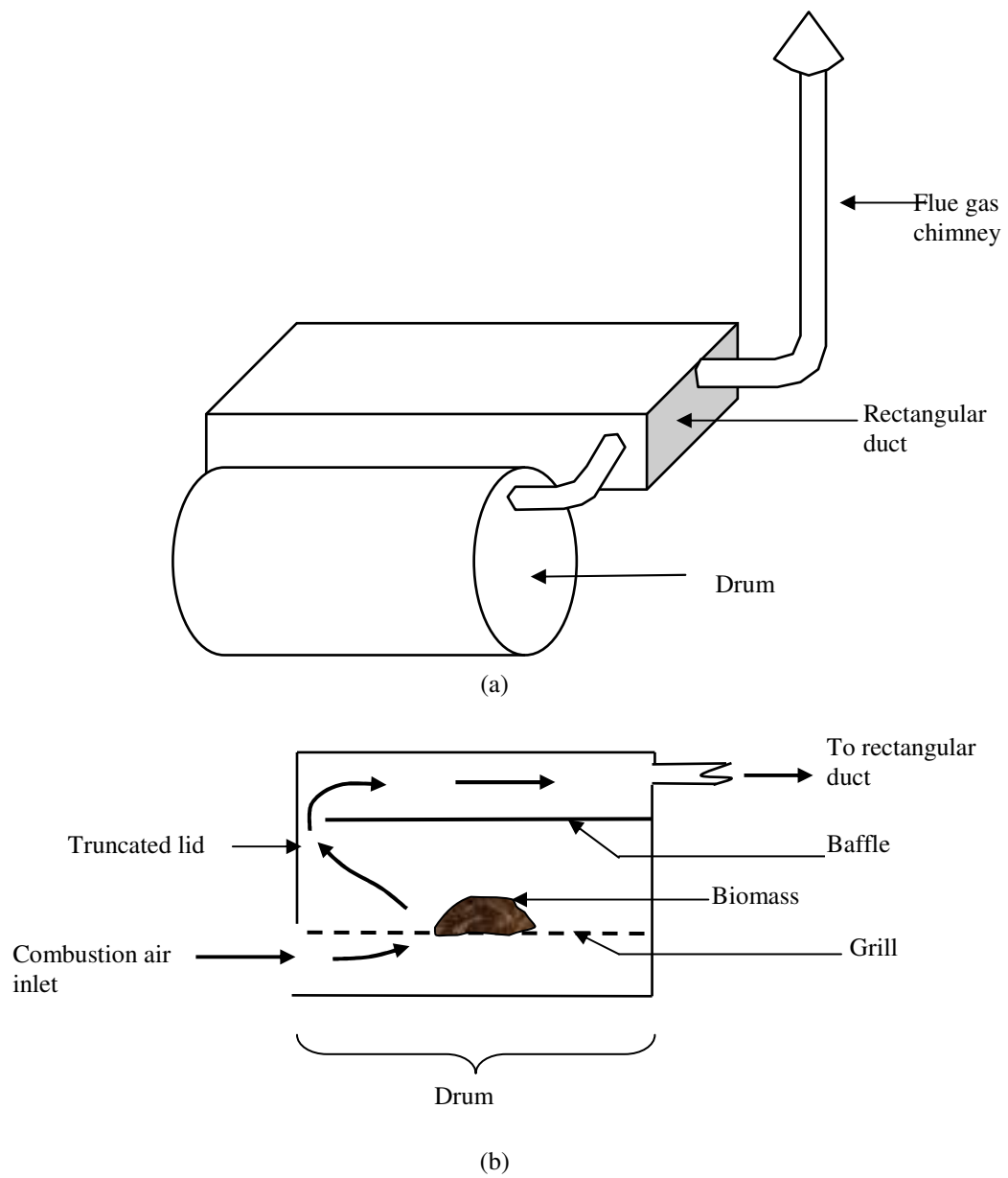


Fig.2: (a) Perspective view of biomass burner, showing drum, rectangular duct and flue gas chimney, b) longitudinal sectional view of the drum, showing flow pattern of flue gas.

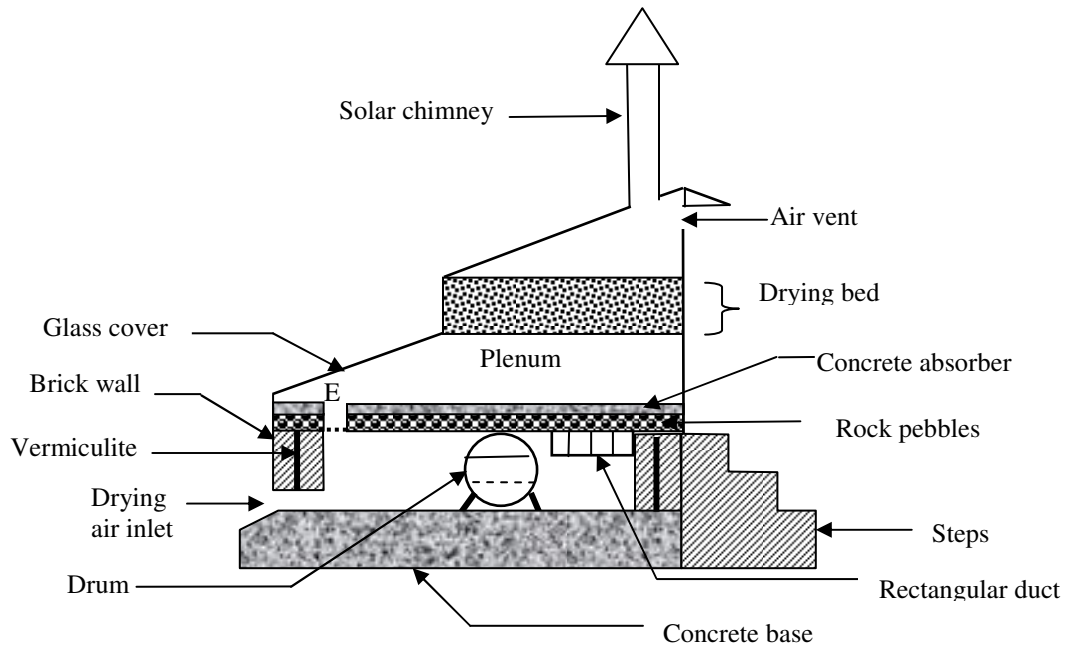


Fig. 3: Description of the components of the solar dryer viewed across the burner, drying chamber and solar chimney.

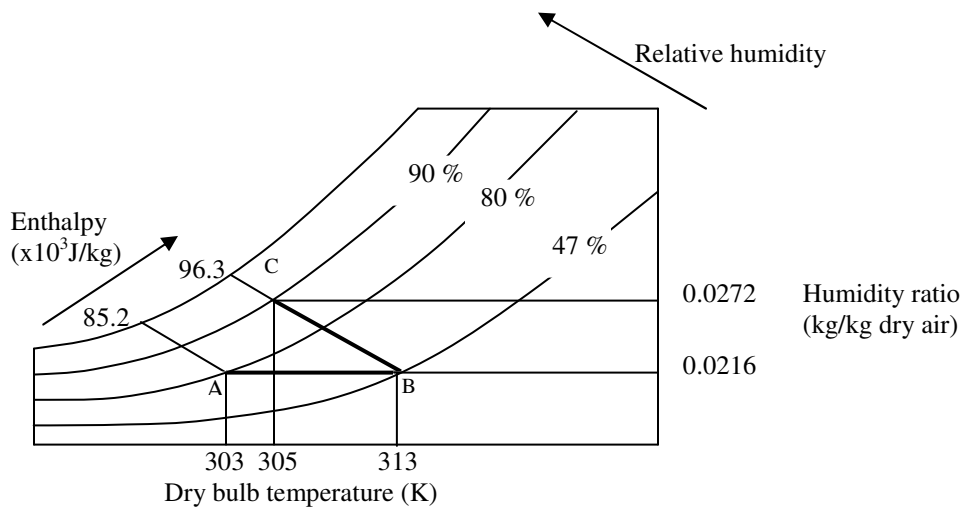


Fig.4: Illustration of psychrometric drying: Air is heated at constant humidity ratio in the solar collector from point A to point B, and it passes through the drying bed isenthalpically from point B to point C.

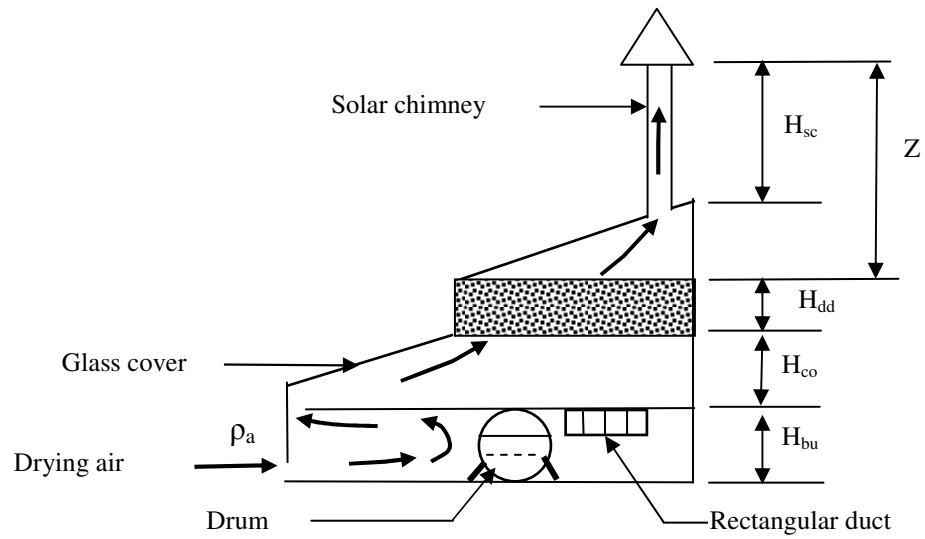


Fig.5: Cross-sectional view of the solar dryer; showing flow of drying air through the biomass burner housing, drying chamber and solar chimney. $H_{bu} = 0.59$ m, $H_{co} = 0.58$ m, $H_{dd} = 0.3$ m, $Z = 1.63$ m and $H_{sc} = 1.2$ m.

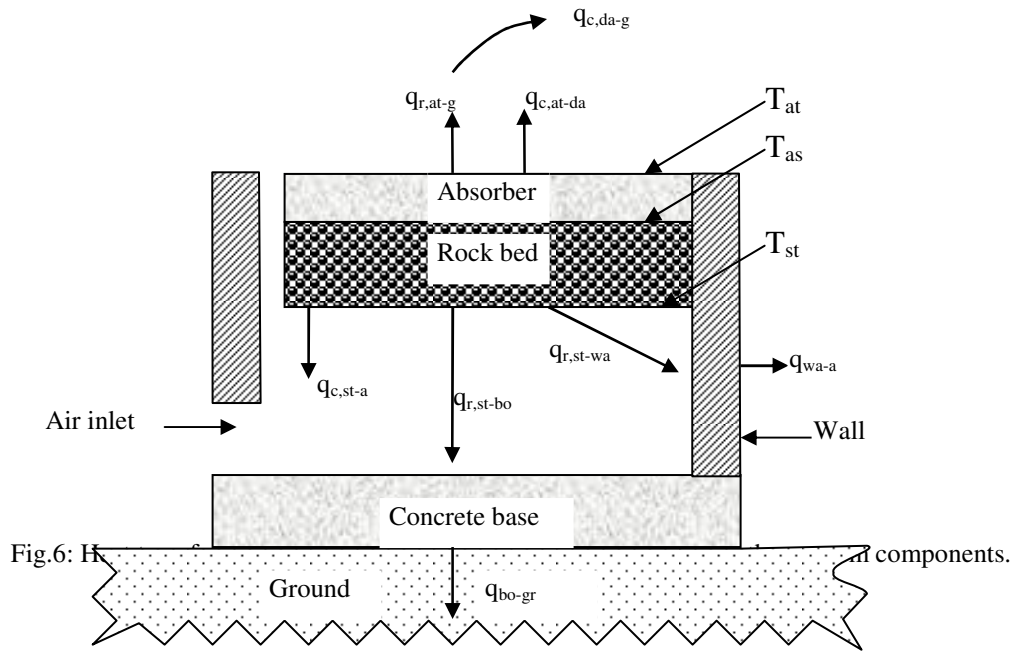


Fig.6: Heat exchanger components.

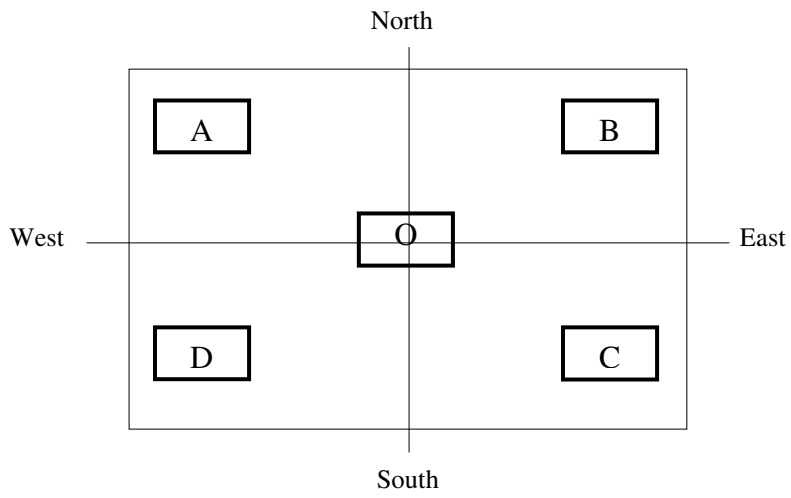
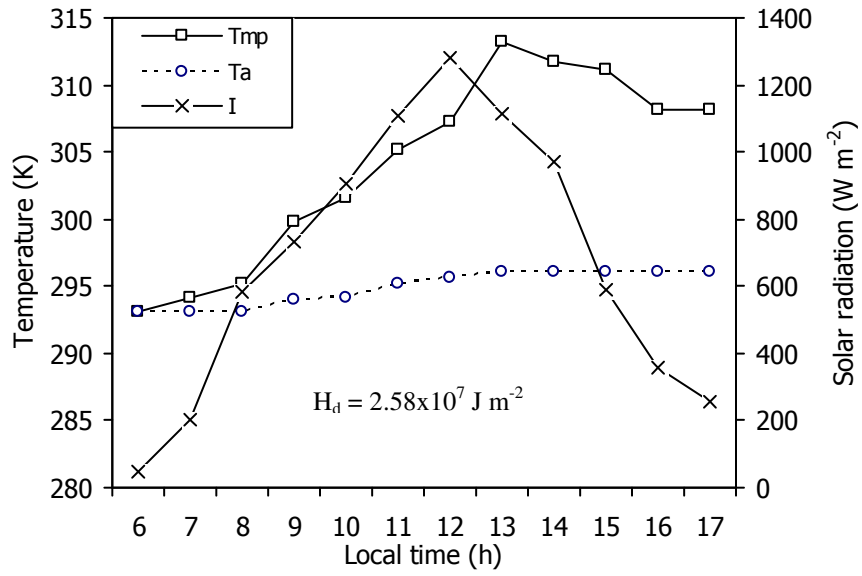
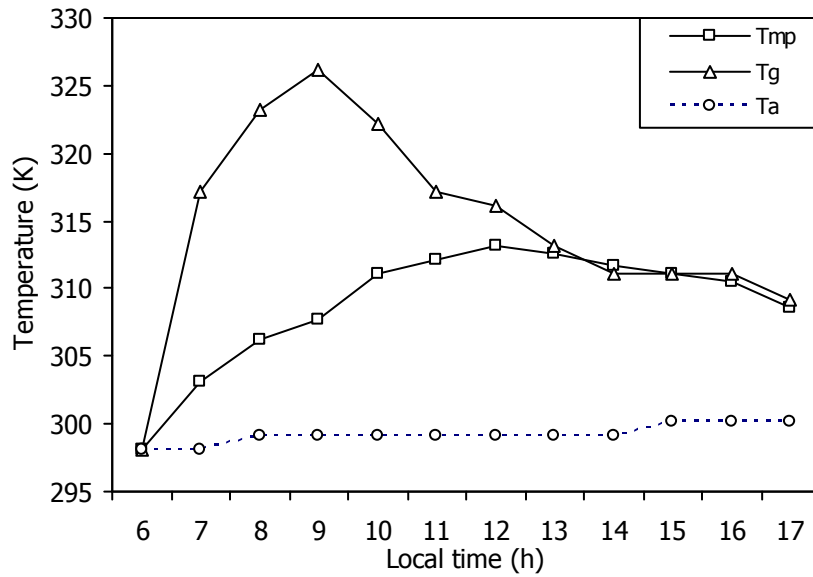


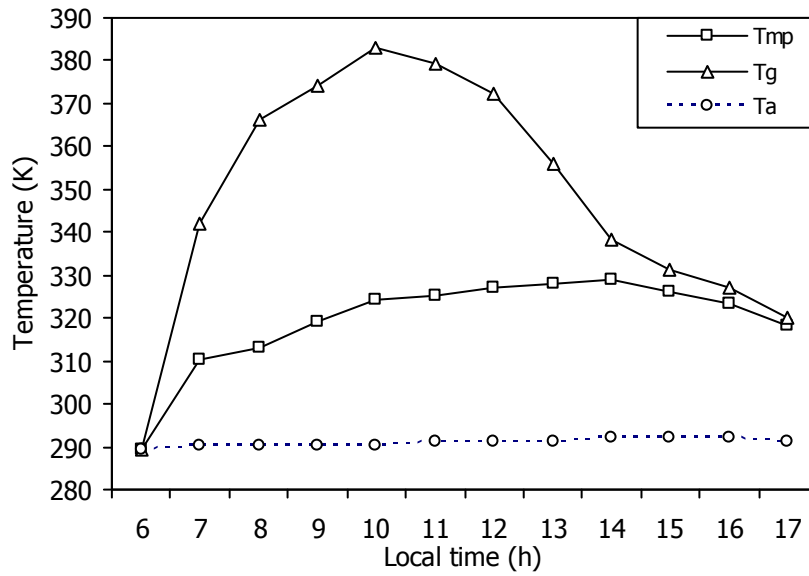
Fig.7: Positions of five pineapple samples used for determination of drying uniformity across the bottom tray.



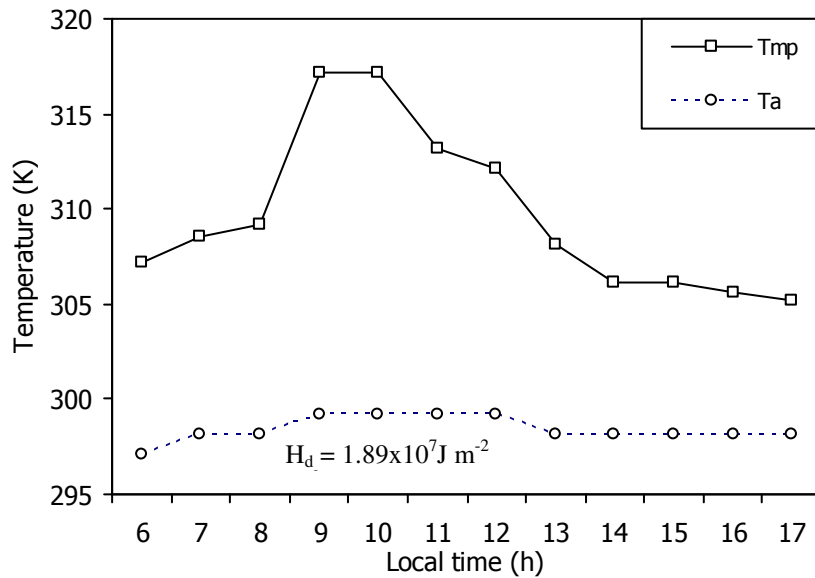
(a)



(b)



(c)



(d)

Fig.8: Variation of mean plenum (T_{pm}), flue gas (T_g) and ambient air (T_a) temperatures, and instantaneous solar irradiation (I) with local time on typical days for different modes of dryer operation: a) solar energy on 28th July, 2004, b) biomass with closed burner door on 30th November, 2004 and c) biomass with open burner door on 21st May, 2004, and d) solar-biomass on 25th February, 2004.

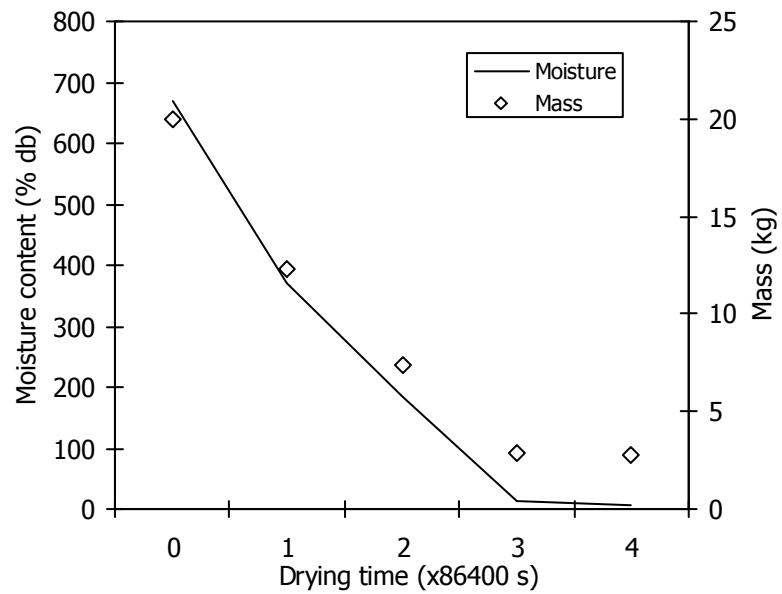


Fig.9: Variation of moisture content (% db) and mass of a typical batch of pineapples (dried from 21st to 24th June 2004 using the solar-biomass mode of operation) with drying time.

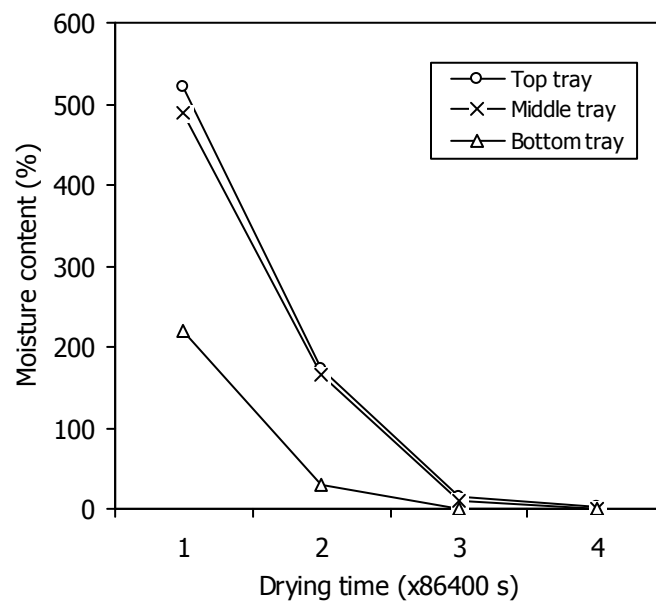


Fig. 10: Variation of moisture content at different trays (batch dried from 28th June to 1st July 2004 using the solar-biomass mode of operation).

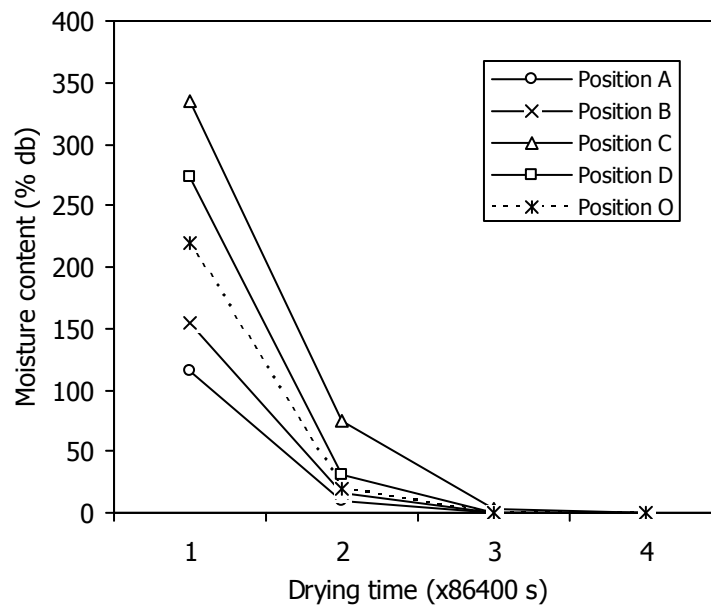


Fig.11: Uniformity of drying rate across the bottom tray (batch dried from 28th June to 1st July 2004 using the solar-biomass mode of operation).